Linear Quadratic Pursuit and Evasion Differential Game Guidance Strategy with Obstacle Avoidance

Xintao WANG, Ming YANG, Ping MA, Tao CHAO*

Control and Simulation Center, Harbin Institute of Technology, Harbin 150080, China

National Key Laboratory of Complex System Control and Intelligent Agent Cooperation, Harbin 150080, China

Abstract: In this paper, a class of linear quadratic differential game guidance scheme is presented to study the pursuit and evasion conflict scenario that an evader establishes a static obstacle and performs the evasion maneuver to avoid a pursuer. First of all, the engagement kinematic model among the obstacle, the pursuer, and the evader is linearized according to the assumption. The issue of the pursuit and evasion game is transformed into a linear quadratic differential game through the dead zone and the cost functions. Furthermore, the linear quadratic differential game approach is utilized to obtain the guidance strategy with obstacle avoidance. Numerical simulation results are employed to validate the performance of the guidance policy.

Keywords: Linear Quadratic Differential Game theory, Obstacle Avoidance, Pursuit and Evasion, Guidance Strategy, Dead Zone Function

1. Introduction

The pursuit and evasion game engagement has received more attention in recent years. An aircraft (evader) performs the evasion maneuver to avoid the interception of the incoming vehicle (pursuer), which is a two-player zero-sum game. Linear quadratic differential game theory^[1] was founded to study the combat issue of pursuit and evasion. Attack active defense aircraft guidance strategy was presented in [2] to address the game problem from the perspective of the pursuer. Based on the above research, combined and cooperative guidance algorithms were derived and considered minimum-effort constraints for active aircraft defense scenarios. A combined linear-quadratic/norm-bounded differential game guidance scheme was devised by Turetsky et al.^[3] for a one-on-one game confrontation scenario. Yan et al.^[4] investigated an evasion guidance law under the condition of unknown pursuer dynamics. It is significant to note that the pursuit and evasion game problem with obstacle avoidance isn't taken into account in the abovementioned literature.

The optimal guidance method^[5] is introduced to derive the game policy for one-on-one intercept, which avoids the spatial region with minimum effort. Linear-quadratic-based optimal guidance law was presented in [6] to avoid the obstacle and intercept the evader for the rendezvous. A combat environment with several static obstacles was considered by Kumar et al.^[7] to design a novel intercept angle guidance scheme by the optimal control theory. Based on the pursuit and evasion game framework, [8] studied a new engagement scenario of multiple pursuers versus multiple evaders. An innovative performance index with obstacle avoidance was proposed in [9] for the issue of multi-agent cooperation. Energy optimal constraint was satisfied in [10] for spacecraft using proximity approach with obstacle avoidance. The guidance strategies designed in the above paper must impose the assumption of maneuvering form for the evader, however, it is difficult to obtain the guidance scheme of the evader through sensor measurement in actual combat.

In summary, the one-on-one pursuit and evasion game issue with obstacle avoidance is taken into consideration to ensure that the pursuer avoids the static obstacle and attacks the evader. Based on

linear quadratic differential game theory, a novel guidance scheme is designed for the pursuit and evasion game scenario with obstacle avoidance. Proposing the minimum-effort cost function through the dead-zone function obtains the Hamiltonian equation. The avoidance distance is introduced into the guidance strategy as a design parameter to evade the static obstacle with different radii.

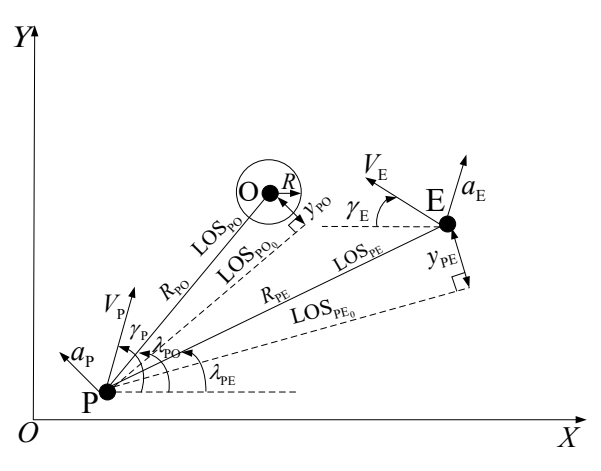


Fig. 1. Kinematic geometry

2.1 Nonlinear kinematics

The engagement relationship of the adversaries is shown in Fig. 1, which is composed of a pursuer (P), an evader (E), and a static obstacle (O). R_i , $i \in \{PE, PO\}$ are the relative distance between the pursuer and the evader; the relative distance between the pursuer and the obstacle. V_i , $i \in \{P, E\}$ represent the velocities of each adversary, respectively. γ_i and λ_i , $i \in \{PE, PO\}$ are the heading angles and line-of-sight (LOS) angles of the pursuer and the evader. R is a minimum avoidance distance of the pursuer evading the obstacle.

The nonlinear model kinematics are

$$\dot{R}_{\rm PE} = V_{\rm P} \cos(\gamma_{\rm P} - \lambda_{\rm PE}) + V_{\rm E} \cos(\gamma_{\rm E} + \lambda_{\rm PE}) \tag{1}$$

$$\dot{\lambda}_{\rm PE} = \frac{V_{\rm E} \sin(\gamma_{\rm E} + \lambda_{\rm PE}) - V_{\rm P} \sin(\gamma_{\rm P} - \lambda_{\rm PE})}{R_{\rm PE}} \tag{2}$$

$$\dot{R}_{\rm PO} = V_{\rm P} \cos(\gamma_{\rm P} - \lambda_{\rm PO}) \tag{3}$$

$$\dot{\lambda}_{\rm PO} = -\frac{V_{\rm P} \sin(\gamma_{\rm P} - \lambda_{\rm PO})}{R_{\rm PO}} \tag{4}$$

The arbitrary-order dynamics of the adversaries is expressed as

$$\dot{\mathbf{x}}_i = \mathbf{A}_i \mathbf{x}_i + \mathbf{b}_i \mathbf{u}_i', \ i \in \{P, E\}$$
 (5)

$$a_i = \mathbf{C}_i \mathbf{x}_i + d_i u_i', \ i \in \{ \mathbf{P}, \mathbf{E} \}$$
 (6)

where x_i is the state vector of each adversary; u'_i is control input of each adversary; A_i , b_i , C_i and d_i are dynamics model matrices of the players.

The flight path angle is represented as

$$\dot{\gamma}_i = \frac{a_i}{V_i}, \ i \in \{P, E\}$$
 (7)

2.2 Linear kinematics

The assumption that the engagement scene is located near the collision triangles and the speeds of the pursuer and the evader are constant is given to linearize the system model. The relative separation between PE and initial line-of-sight LOS_{PE₀} is represented as y_{PE} ; the relative separation between PO and initial line-of-sight LOS_{PO₀} is defined as y_{PO} . u_{PL} and u_{EL} are the acceleration commands normal to initial LOS, respectively. The parameters given in (5) and (6) are chosen as $A_i = 0$, $b_i = 0$, $C_i = 0$, $d_i = 1$, $i \in \{PE, PO\}$ under the assumption of the adversaries with the idea system dynamic. Subscript 0 represents the initial state of the players.

The following equations are acquired based on the linearized framework.

$$\begin{cases} u_{\rm PL} = a_{\rm P} \cos(\gamma_{\rm P_0} - \lambda_{\rm PE_0}) = \cos(\gamma_{\rm P_0} - \lambda_{\rm PE_0}) u_{\rm P}' \\ u_{\rm EL} = a_{\rm E} \cos(\gamma_{\rm E_0} + \lambda_{\rm PE_0}) = \cos(\gamma_{\rm E_0} + \lambda_{\rm PE_0}) u_{\rm E}' \end{cases}$$
(8)

(9) is derived according to above definitions.

$$\begin{cases} u_{P} = \cos(\gamma_{P_{0}} - \lambda_{PE_{0}}) u_{P}' \\ u_{E} = \cos(\gamma_{E_{0}} + \lambda_{PE_{0}}) u_{E}' \end{cases}$$
 (9)

Choose the following state variables of linearized model.

$$\mathbf{x} = \begin{bmatrix} y_{\text{PE}} & \dot{y}_{\text{PE}} & y_{\text{PO}} & \dot{y}_{\text{PO}} \end{bmatrix}^{\text{T}}$$
 (10)

Differentiating the state variable yields the following formulas.

$$\dot{\mathbf{x}} = \begin{cases}
\dot{y}_{PE} = x_2 \\
\ddot{y}_{PE} = u_{EL} - u_{PL} \\
\dot{y}_{PO} = x_4 \\
\ddot{y}_{PO} = -u_{PL}
\end{cases}$$
(11)

The state equation is

$$\dot{\mathbf{x}} = A\mathbf{x} + \mathbf{B}\mathbf{u}_{\scriptscriptstyle \mathrm{F}} + \mathbf{C}\mathbf{u}_{\scriptscriptstyle \mathrm{P}} \tag{12}$$

where

$$\mathbf{A} = \begin{bmatrix} 0 & 1 & 0 & 0 \\ 0 & 0 & 0 & 0 \\ 0 & 0 & 0 & 1 \\ 0 & 0 & 0 & 0 \end{bmatrix}, \quad \mathbf{B} = \begin{bmatrix} 0 & 1 & 0 & 0 \end{bmatrix}^{\mathrm{T}}, \quad \mathbf{C} = \begin{bmatrix} 0 & -1 & 0 & -1 \end{bmatrix}^{\mathrm{T}}$$

The terminal time among the pursuer, the obstacle and the evader are defined as follows.

$$t_i^f = \frac{R_i}{\dot{R}_i}, \quad i \in \{ \text{PE}, \text{PO} \}$$
 (13)

and satisfy $t_{PO}^f < t_{PE}^f$.

According to above definition, the time-to-go of the adversaries are given as

$$t_i^{go} = t_i^f - t, \quad i \in \{\text{PE}, \text{PO}\}$$
 (14)

The interval of the terminal time is defined as

$$\Delta = t_{\rm PE}^f - t_{\rm PO}^f \tag{15}$$

3. Problem Formulation

Zero-effort miss (ZEM) is introduced to reduce the system order, which is the miss distance if none of the adversaries in engagement apply any control from the current time onward. The ZEMs between the pursuer-obstacle and the pursuer-evader are expressed as Z_{PO} and Z_{PE} .

3.1 Order Reduction

 Z_{PO} and Z_{PE} are represented as the following forms by virtue of terminal projection transformation.

$$\begin{cases}
Z_{PO} = \boldsymbol{\eta}_{PO} \boldsymbol{\phi}(t_{PO}^{f}, t) \boldsymbol{x} \\
Z_{PE} = \boldsymbol{\eta}_{PE} \boldsymbol{\phi}(t_{PE}^{f}, t) \boldsymbol{x}
\end{cases} \tag{16}$$

where η_{PO} and η_{PE} are

$$\begin{cases} \boldsymbol{\eta}_{PO} = \begin{bmatrix} 0 & 0 & 1 & 0 \end{bmatrix} \\ \boldsymbol{\eta}_{PE} = \begin{bmatrix} 1 & 0 & 0 & 0 \end{bmatrix}$$

and the state-transition matrices $\phi(t_{PO}^f, t)$ and $\phi(t_{PE}^f, t)$ are

$$\phi(t_i^f, t) = \begin{bmatrix} 1 & t_i^{go} & 0 & 0 \\ 0 & 1 & 0 & 0 \\ 0 & 0 & 1 & t_i^{go} \\ 0 & 0 & 0 & 1 \end{bmatrix}, i \in \{\text{PE, PO}\}$$
(17)

Formula (16) is rewritten as

$$\begin{cases} Z_{PO} = y_{PO} + \dot{y}_{PO} t_{PO}^{go} \\ Z_{PE} = y_{DE} + \dot{y}_{PE} t_{PE}^{go} \end{cases}$$
(18)

Take the derivative of (18) to obtain the following formulas.

$$\begin{cases} \dot{Z}_{PO} = -u_P t_{PO}^{go} \\ \dot{Z}_{PE} = (u_E - u_P) t_{PE}^{go} \end{cases}$$
(19)

Remark 1. The order of x is changed from 4 to 1, which reduces the complexity of the game problem.

The following cost function is obtained according to the above analysis.

$$J = \left| D \left[Z_{PO}(t_{PO}^f) \right] \right|^2 + \left| Z_{PE}(t_{PE}^f) \right|^2 + \alpha_P \int_t^{t_{PE}^f} u_P^2(\varepsilon) d\varepsilon - \alpha_E \int_t^{t_{PE}^f} u_E^2(\varepsilon) d\varepsilon$$
 (20)

where α_P and α_E are the weight parameters, $D[\bullet]$ is the dead-zone function to avoid the static obstacle and the specific form is

$$\mathbf{D} \begin{bmatrix} Z_{\text{PO}}(t_{\text{PO}}^f) \end{bmatrix} = \begin{cases} 0, & \left| Z_{\text{PO}}(t_{\text{PO}}^f) \right| \ge R \\ \left[Z_{\text{PO}}(t_{\text{PO}}^f) - R \right], & 0 \le Z_{\text{PO}}(t_{\text{PO}}^f) < R \\ \left[Z_{\text{PO}}(t_{\text{PO}}^f) + R \right], & -R < Z_{\text{PO}}(t_{\text{PO}}^f) < 0 \end{cases}$$

4. Guidance Scheme

According to (20), the Hamiltonian function is given as follow.

$$H = \lambda_{\rm PO} \dot{\mathbf{D}} \left[Z_{\rm PO}(t) \right] + \lambda_{\rm PE} \dot{Z}_{\rm PE}(t) + \alpha_{\rm P} u_{\rm P}^2(t) - \alpha_{\rm E} u_{\rm E}^2(t) \tag{21}$$

The adjoint equation and transversality conditions are

$$\begin{cases}
\dot{\lambda}_{PO} = -\frac{\partial H}{\partial D[Z_{PO}(t)]} = 0 \\
\dot{\lambda}_{PE} = -\frac{\partial H}{\partial Z_{PE}(t)} = 0
\end{cases},
\begin{cases}
\lambda_{PO}(t_{PO}^{f}) = \frac{\partial J}{\partial D[Z_{PO}(t_{PO}^{f})]} = 2D[Z_{PO}(t_{PO}^{f})] \\
\lambda_{PE}(t_{PE}^{f}) = \frac{\partial J}{\partial Z_{PE}(t_{PE}^{f})} = 2Z_{PE}(t_{PE}^{f})
\end{cases} (22)$$

Bringing $\dot{D}[Z_{PO}(t)]$ and equation (22) into (21) obtains

$$H = 2D \left[Z_{PO}(t_{PO}^f) \right] \dot{Z}_{PO}(t) + 2Z_{PE}(t_{PE}^f) \dot{Z}_{PE}(t) + \alpha_p u_P^2(t) - \alpha_E u_E^2(t)$$
(23)

Substitute (19) into (23) to yield the following formula.

$$H = -2D \left[Z_{PO}(t_{PO}^{f}) \right] t_{PO}^{go} u_{P}(t) + 2Z_{PE}(t_{PE}^{f}) t_{PE}^{go} \left[u_{E}(t) - u_{P}(t) \right] + \alpha_{P} u_{P}^{2}(t) - \alpha_{E} u_{E}^{2}(t)$$

$$= 2Z_{PE}(t_{PE}^{f}) t_{PE}^{go} u_{E}(t) - 2 \left[D \left[Z_{PO}(t_{PO}^{f}) \right] t_{PO}^{go} + Z_{PE}(t_{PE}^{f}) t_{PE}^{go} \right] u_{P}(t) + \alpha_{P} u_{P}^{2}(t) - \alpha_{E} u_{E}^{2}(t)$$
(24)

The open-loop optimal guidance schemes are acquired by minimizing the Hamiltonian function (24).

$$u_{\rm p}^* = \frac{D[Z_{\rm PO}(t_{\rm PO}^f)]t_{\rm PO}^{go} + Z_{\rm PE}(t_{\rm PE}^f)t_{\rm PE}^{go}}{\alpha_{\rm p}}, \quad u_{\rm E}^* = \frac{Z_{\rm PE}(t_{\rm PE}^f)t_{\rm PE}^{go}}{\alpha_{\rm E}}$$
(25)

Substituting (25) into (19) and integrating from t to t_{PO}^f , we get

$$Z_{PO}(t_{PO}^{f}) - Z_{PO}(t) = -\frac{D\left[Z_{PO}(t_{PO}^{f})\right] \int_{t}^{t_{PO}^{f}} t_{PO}^{go^{2}}(\varepsilon) d\varepsilon}{\alpha_{P}} - \frac{Z_{PE}(t_{PE}^{f}) \int_{t}^{t_{PO}^{f}} t_{PO}^{go}(\varepsilon) t_{PE}^{go}(\varepsilon) d\varepsilon}{\alpha_{P}}$$

$$= -\frac{D\left[Z_{PO}(t_{PO}^{f})\right] t_{PO}^{go^{3}}}{3\alpha_{P}} - \frac{Z_{PE}(t_{PE}^{f}) t_{PO}^{go^{2}}(3\Delta + 2t_{PO}^{go})}{6\alpha_{P}}$$
(26)

(26) can be rewritten as

$$Z_{PO}(t_{PO}^{f}) + \frac{D\left[Z_{PO}(t_{PO}^{f})\right]t_{PO}^{go3}}{3\alpha_{P}} = Z_{PO}(t) - \frac{Z_{PE}(t_{PE}^{f})t_{PO}^{go2}(3\Delta + 2t_{PO}^{go})}{6\alpha_{P}}$$

According to the $D[\cdot]$, the following equation is derived.

$$Z_{PO}(t_{PO}^{f}) = \begin{cases} Z_{PO}(t) - \frac{t_{PO}^{go^{2}}(3\Delta + 2t_{PO}^{go})}{2(3\alpha_{P} + t_{PO}^{go^{3}})} Z_{PE}(t_{PE}^{f}), & \left| Z_{PO}(t_{PO}^{f}) \right| \ge R \\ \frac{3\alpha_{P}Z_{PO}(t) + t_{PO}^{go^{3}}R}{3\alpha_{P} + t_{PO}^{go^{3}}} - \frac{t_{PO}^{go^{2}}(3\Delta + 2t_{PO}^{go})}{2(3\alpha_{P} + t_{PO}^{go^{3}})} Z_{PE}(t_{PE}^{f}), & 0 \le Z_{PO}(t_{PO}^{f}) < R \\ \frac{3\alpha_{P}Z_{PO}(t) - t_{PO}^{go^{3}}R}{3\alpha_{P} + t_{PO}^{go^{3}}} - \frac{t_{PO}^{go^{2}}(3\Delta + 2t_{PO}^{go})}{2(3\alpha_{P} + t_{PO}^{go^{3}})} Z_{PE}(t_{PE}^{f}), & -R < Z_{PO}(t_{PO}^{f}) < 0 \end{cases}$$

$$(27)$$

Bringing (27) into the dead-zone function $D[\bullet]$, we get

$$\begin{split} \mathbf{D} \Big[Z_{\text{PO}}(t_{\text{PO}}^f) \Big] = & \begin{cases} -\frac{t_{\text{PO}}^{go^2}(3\Delta + 2t_{\text{PO}}^{go})}{2(3\alpha_{\text{P}} + t_{\text{PO}}^{go^3})} Z_{\text{PE}}(t_{\text{PE}}^f), & \left| Z_{\text{PO}}(t) \right| \geq R \\ \frac{6\alpha_{\text{P}} \left[Z_{\text{PO}}(t) - R \right] - t_{\text{PO}}^{go^2}(3\Delta + 2t_{\text{PO}}^{go}) Z_{\text{PE}}(t_{\text{PE}}^f)}{2(3\alpha_{\text{P}} + t_{\text{PO}}^{go^3})}, & 0 \leq Z_{\text{PO}}(t) < R \\ \frac{6\alpha_{\text{P}} \left[Z_{\text{PO}}(t) + R \right] - t_{\text{PO}}^{go^2}(3\Delta + 2t_{\text{PO}}^{go}) Z_{\text{PE}}(t_{\text{PE}}^f)}{2(3\alpha_{\text{P}} + t_{\text{PO}}^{go^3})}, & -R < Z_{\text{PO}}(t) < 0 \end{cases} \end{split}$$

$$= \frac{3\alpha_{\rm p} D[Z_{\rm PO}(t)]}{3\alpha_{\rm p} + t_{\rm PO}^{go3}} - \frac{t_{\rm PO}^{go3} (3\Delta + 2t_{\rm PO}^{go}) Z_{\rm PE}(t_{\rm PE}^f)}{2(3\alpha_{\rm p} + t_{\rm PO}^{go3})}$$
(28)

Similarly, substituting (25) into (19), and integrating from t to t_{PE}^f yield

$$Z_{PE}(t_{PE}^{f}) - Z_{PE}(t) = \int_{t}^{t_{PE}} \frac{Z_{PE}(t_{PE}^{f})t_{PE}^{go2}(\varepsilon)}{\alpha_{E}}$$

$$- \frac{D\left[Z_{PO}(t_{PO}^{f})\right]t_{PO}^{go}(\varepsilon)t_{PE}^{go}(\varepsilon) + Z_{PE}(t_{PE}^{f})t_{PE}^{go2}(\varepsilon)}{\alpha_{P}} d\varepsilon$$

$$= \frac{Z_{PE}(t_{PE}^{f})(\alpha_{P} - \alpha_{E})\int_{t}^{t_{PE}^{f}}t_{PE}^{go2}(\varepsilon)d\varepsilon}{\alpha_{P}\alpha_{E}} - \frac{D\left[Z_{PO}(t_{PO}^{f})\right]\int_{t}^{t_{PE}^{f}}t_{PO}^{go}(\varepsilon)t_{PE}^{go}(\varepsilon)d\varepsilon}{\alpha_{P}}$$

$$= \frac{t_{PE}^{go3}(\alpha_{P} - \alpha_{E})Z_{PE}(t_{PE}^{f})}{3\alpha_{P}\alpha_{P}} - \frac{t_{PE}^{go2}(2t_{PE}^{go} - 3\Delta)D\left[Z_{PO}(t_{PO}^{f})\right]}{6\alpha_{P}}$$
(29)

Equation (29) becomes

$$Z_{PE}(t_{PE}^{f}) = \frac{3\alpha_{P}\alpha_{E}Z_{PE}(t)}{3\alpha_{P}\alpha_{E} - (\alpha_{P} - \alpha_{E})t_{PE}^{go3}} - \frac{\alpha_{E}t_{PE}^{go2}(2t_{PE}^{go} - 3\Delta)D[Z_{PO}(t_{PO}^{f})]}{6\alpha_{P}\alpha_{E} - 2(\alpha_{P} - \alpha_{E})t_{PE}^{go3}}$$
(30)

Combining (28) and (30), we obtain the following formulas.

$$Z_{\text{PE}}(t_{\text{PE}}^{f}) = \frac{12\alpha_{\text{P}}\alpha_{\text{E}}(3\alpha_{\text{P}} + t_{\text{PO}}^{go3})Z_{\text{PE}}(t) - 6\alpha_{\text{P}}\alpha_{\text{E}}t_{\text{PE}}^{go3}(2t_{\text{PE}}^{go} - 3\Delta)D[Z_{\text{PO}}(t)]}{6\alpha_{\text{P}}^{2}\alpha_{\text{E}} + 12\alpha_{\text{P}}\alpha_{\text{E}}(t_{\text{PE}}^{go} + t_{\text{PO}}^{go})(\Delta^{2} + t_{\text{PE}}^{go}t_{\text{PO}}^{go}) - 4\alpha_{\text{P}}t_{\text{PE}}^{go3}(3 + t_{\text{PO}}^{go3}) + 3\alpha_{\text{E}}\Delta^{2}t_{\text{PO}}^{go2}t_{\text{PE}}^{go2}}$$
(31)

$$D[Z_{PO}(t_{PO}^f)] = \frac{\left[36\alpha_{P}^2\alpha_{E} - 12\alpha_{P}t_{PE}^{go3}(\alpha_{P} - \alpha_{E})\right]D[Z_{PO}(t)] - 6\alpha_{P}\alpha_{E}t_{PO}^{go2}(3\Delta + 2t_{PO}^{go})Z_{PE}(t)}{6\alpha_{P}^2\alpha_{E} + 12\alpha_{P}\alpha_{E}(t_{EP}^{go} + t_{PO}^{go})(\Delta^2 + t_{EO}^{go}t_{PO}^{go}) - 4\alpha_{P}t_{EP}^{go3}(3 + t_{EO}^{go3}) + 3\alpha_{E}\Delta^2t_{EO}^{go2}t_{EP}^{go2}}$$
 (32)

The closed-loop optimal guidance strategies of the adversaries are derived by substituting (31) and (32) into (25).

$$u_{\rm p}^* = \frac{\left[(4\alpha_{\rm E} - \alpha_{\rm p}) t_{\rm pE}^{go3} t_{\rm pO}^{go} - \alpha_{\rm E} (t_{\rm pE}^{go3} \Delta + 6\alpha_{\rm p} t_{\rm pO}^{go}) \right] D[Z_{\rm pO}(t)] + 6\alpha_{\rm E} (t_{\rm pO}^{go3} \Delta - 6\alpha_{\rm E}) Z_{\rm pE}(t)}{6\alpha_{\rm p}^2 \alpha_{\rm E} + 12\alpha_{\rm p} \alpha_{\rm E} (t_{\rm pE}^{go} + t_{\rm pO}^{go}) (\Delta^2 + t_{\rm pE}^{go3} t_{\rm pO}^{go}) - 4\alpha_{\rm p} t_{\rm pE}^{go3} (3 + t_{\rm pO}^{go3}) + 3\alpha_{\rm E} \Delta^2 t_{\rm pO}^{go2} t_{\rm pe}^{go2}}$$
(33)

$$u_{\rm E}^* = \frac{12\alpha_{\rm p}t_{\rm PE}^{go}(3\alpha_{\rm p} + t_{\rm PO}^{go3})Z_{\rm PE}(t) - 6\alpha_{\rm p}t_{\rm PE}^{go3}(2t_{\rm PE}^{go} - 3\Delta)D[Z_{\rm PO}(t)]}{6\alpha_{\rm p}^2\alpha_{\rm E} + 12\alpha_{\rm p}\alpha_{\rm E}(t_{\rm PE}^{go} + t_{\rm PO}^{go})(\Delta^2 + t_{\rm PE}^{go}t_{\rm PO}^{go}) - 4\alpha_{\rm p}t_{\rm PE}^{go3}(3 + t_{\rm PO}^{go3}) + 3\alpha_{\rm E}\Delta^2t_{\rm PO}^{go2}t_{\rm PE}^{go2}}$$
(34)

Remark 2: The following constraints must be satisfied for the sake of the effectiveness of guidance strategies (33) and (34).

$$\frac{\partial Z_{PO}(t_{PO}^{f})}{\partial Z_{PO}(t)} = \begin{cases}
1, & \left| Z_{PO}(t_{PO}^{f}) \right| \ge R \\
\frac{3\alpha_{P}}{3\alpha_{P} + t_{PO}^{g\sigma^{3}}}, & 0 \le Z_{PO}(t_{PO}^{f}) < R \\
\frac{3\alpha_{P}}{3\alpha_{P} + t_{PO}^{g\sigma^{3}}}, & -R < Z_{PO}(t_{PO}^{f}) < 0
\end{cases}$$
(35)

Since

$$\frac{3\alpha_{\rm p}}{3\alpha_{\rm p} + t_{\rm PO}^{go3}} > 0 \tag{36}$$

 $\frac{1}{3\alpha_{\rm p} + t_{\rm PO}^{go3}} > 0$ Then, for $\left| Z_{\rm PO}(t_{\rm PO}^f) \right| \ge R$, $\left| Z_{\rm PO}(t) \right| \ge R$; for $0 \le Z_{\rm PO}(t_{\rm PO}^f) < R$, $0 \le Z_{\rm PO}(t) < R$; for $-R < Z_{PO}(t_{PO}^f) < 0$.

5. Simulations

The effectiveness of the guidance scheme proposed in this paper is validated by nonlinear numerical simulations. The engagement that the pursuer evades the static obstacle and hits the evader is supposed in this section. The assumption of the information required in the guidance strategy being measured is given. Three minimum avoidance values: 0m (no avoidance), 200m, and 400m are chosen in Cases 1 and 2 to verify the guidance scheme with obstacle avoidance.

The objective of the nonlinear form of ZEM given in [11] is to improve the accuracy of the simulations.

$$Z_{i}(t) = \dot{R}_{i} t_{i}^{go2} \dot{\lambda}_{i}, j \in \{ \text{PE, PO} \}$$

$$(37)$$

Case 1. The simulation parameters are obtained as follows.

Table 1. Simulation parameters.

Parameters	Pursuer	Evader
Initial Position/km	(10,200)	(110,200)
Initial course/(°)	21	72
Velocity/(km/s)	3.3	1.5

The position of the static obstacle is selected as $x_0 = 67.8920 \text{km}$, $y_0 = 222.0800 \text{km}$. The weight parameters are $\alpha_{\rm P}=0.1$ and $\alpha_{\rm E}=0.01$. The final time are calculated as $t_{\rm PO}^f=20.1115{\rm s}$ and $t_{\rm PE}^f = 28.2140 {\rm s}$.

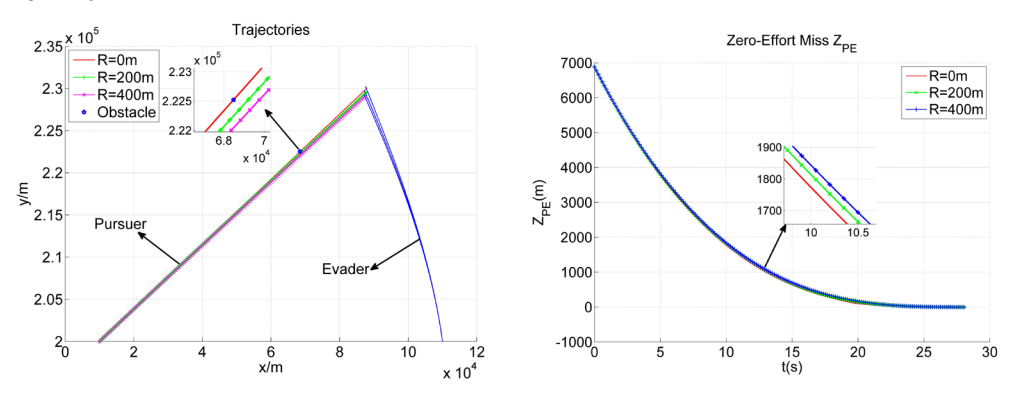


Fig. 1. Engagement trajectories of the guidance scheme Fig. 2. ZEM with respect to the obstacle radius for time

Fig. 1 shows the flight trajectories of the adversaries for the different obstacle radius. It can be seen from Fig. 1 that the pursuer is able to evade the static obstacle with the specific ZEM and intercept the evader.

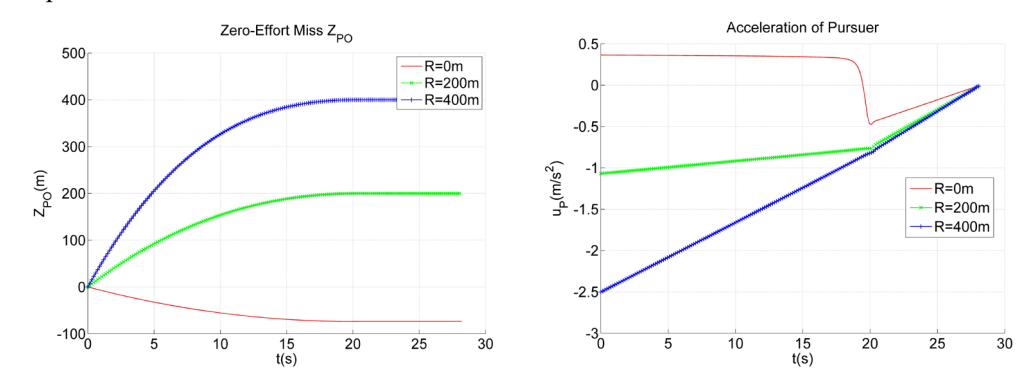


Fig. 3. Engagement trajectories of the guidance scheme Fig. 4. ZEM with respect to the obstacle radius for time. The time evolutions of $Z_{\rm PO}$ and $Z_{\rm PE}$ for the different obstacle avoidance distance are illustrated by Figs. 3 and 4. From Fig. 3 it can be known that the pursuer evades the static obstacle with the specific ZEM for the different obstacle radius at the final time. As shown in Fig. 4, the ZEM between the pursuer and the evader decreases to 0m for the different value of the obstacle radius at the terminal time $t_{\rm PE}^f$, which demonstrates that the pursuer is able to hit the evader and complete the attack mission.

The variation tendency of the acceleration command with respect to time for the different obstacle radius is shown in Fig. 4. The initial value of the pursuer's acceleration gradually increases as the obstacle radius increases, and $u_{\rm p}$ converges to $0 \, {\rm m/s^2}$ at the terminal time in order to guarantee that the pursuer accomplishes the attacking task.

Case 2. The simulation parameters are obtained as follows.

 Parameters
 Pursuer
 Evader

 Initial Position/km
 (5,200)
 (100,200)

 Initial course/(°)
 26
 62

 Velocity/(km/s)
 2.8
 1.5

Table 2. Simulation parameters.

We suppose that the static obstacle is located in $x_0 = 45.2397 \,\mathrm{km}$, $y_0 = 219.6287 \,\mathrm{km}$ The parameters are $\alpha_\mathrm{P} = 1.1$ and $\alpha_\mathrm{E} = 0.01$. The terminal time are calculated as $t_\mathrm{PO}^f = 17.7911 \,\mathrm{s}$ and $t_\mathrm{PE}^f = 29.4955 \,\mathrm{s}$.

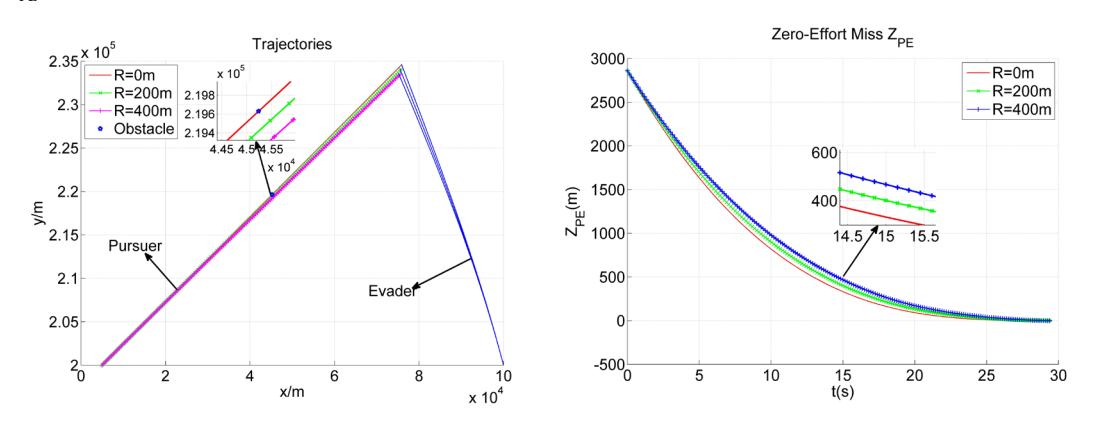


Fig. 5. Engagement trajectories of the guidance scheme Fig. 6. ZEM with respect to the obstacle radius for time

The flight trajectories of the guidance strategy for the adversaries are shown in Fig. 5, which demonstrates that the pursuer evades the static obstacle with different avoidance value and intercepts the evaders.

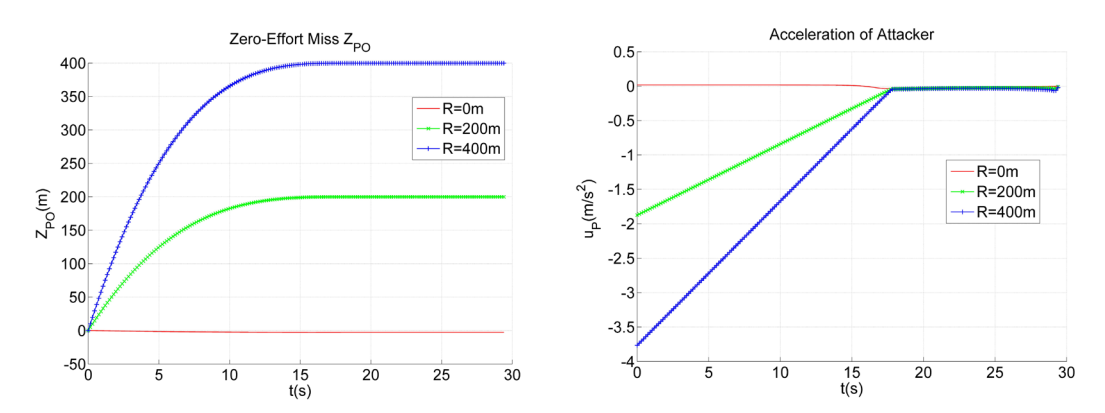


Fig. 7. Engagement trajectories of the guidance scheme Fig. 8. ZEM with respect to the obstacle radius for time Figs. 6 and 7 illustrate the variation tendency of ZEMs among the pursuer, the obstacle and the evader with respect to time. For the different minimum avoidance distance, Z_{PE} decreases and converges to 0m at the final time, which validates the simulation result in Fig. 5. As shown in Fig.

6, Z_{PO} increases and maintains the avoidance value at the terminal time t_{PO}^f , which is consistent with the line in Fig. 6.

The time evolution of the acceleration u_p for the different avoidance distance is shown in Fig. 8. The initial value of the acceleration command increases according to the obstacle radius and u_p converges to 0m/s^2 , which guarantees the success of the attack mission.

6. Conclusion

A framework of one-on-one pursuit and evasion game with the static obstacle is considered by virtue of linear quadratic differential game theory. The differential game guidance scheme is proposed to guarantee that the pursuer avoids the static obstacle and attacks the evader The parameter of the static obstacle radius is taken into consideration in the guidance strategy, which ensures that the pursuer evades the obstacle with the different avoidance value and accomplishes the engagement mission. The performance of the guidance strategy is verified by numerical simulations.

Acknowledgements

This work is supported by National Natural Science Foundation (NNSF) of China under Grant 62273119.

Declaration of Interest

The authors declare that they have no known competing financial interests or personal relationships that could have appeared to influence the work reported in this paper.

Copyright Statement

The authors confirm that they, and/or their company or organization, hold copyright on all of the

original material included in this paper. The authors also confirm that they have obtained permission, from the copyright holder of any third party material included in this paper, to publish it as part of their paper. The authors confirm that they give permission, or have obtained permission from the copyright holder of this paper, for the publication and distribution of this paper as part of the ICAS proceedings or as individual off-prints from the proceedings.

Reference

- [1] V. Shaferman, T. Shima, "Linear Quadratic Guidance Laws for Imposing a Terminal Intercept Angle[J]", Journal of Guidance, Control, and Dynamics, Vol. 31, No. 5, pp. 1400-1412, 2008.
- [2] H. Z. Liang, J. Y. Wang, Y. H. Wang, et al., "Optimal guidance against active defense ballistic missiles via differential game strategies[J]", Chinese Journal of Aeronautics, Vol. 33, No. 3, pp. 978-989, 2020.
- [3] V. Turetsky, M. Weiss, T. Shima, "A combined linear–quadratic/bounded control differential game guidance law[J]", IEEE Transactions on Aerospace and Electronic Systems, Vol. 57, No. 5, pp. 3452-3462, 2021.
- [4] T. Yan, Y. L. Cai, B. Xu, "Evasion guidance for air-breathing hypersonic vehicles against unknown pursuer dynamics[J]", Neural Computing and Applications, 2021.
- [5] T. Shima, "Optimal cooperative pursuit and evasion strategies against a homing missile[J]", Journal of Guidance, Control, and Dynamics, Vol. 34, No. 2, pp. 414-425, 2011.
- [6] M. Weiss, T. Shima, "Linear quadratic optimal control-based missile guidance law with obstacle avoidance[J]", IEEE Transactions on Aerospace and Electronic Systems, Vol. 55, No. 1, pp. 205-214, 2019.
- [7] S. Kumar, M. Weiss, T. Shima, "Minimum-effort intercept angle guidance with multiple-obstacle avoidance[J]", Journal of Guidance, Control, and Dynamics, Vol. 41, No. 6, pp. 1355-1369, 2018.
- [8] B. Jha, R. Tsalik, M. Weiss, et al., "Cooperative guidance and collision avoidance for multiple pursuers[J]", Journal of Guidance, Control, and Dynamics, Vol. 42, No. 7, pp. 1506-1518, 2019.
- [9] J. L. Sun, C. S. Liu, et al., "Optimal obstacle avoidance via distributed consensus algorithms with communication delay[J]", Journal of Systems Engineering and Electronics, Vol. 27, No. 6, pp. 1272-1282, 2016.
- [10] D. Ye, J. Y. Sun, Y. Xiao, et al., "Energy optimal guidance for proximity approach with obstacle avoidance[J]", Aerospace Science and Technology, Vol. 130, pp. 107949, 2022.
- [11] J. Shinar, V. Y. Glizer, V. Turetsky, "The effect of pursuer dynamics on the value of linear pursuit-evasion games with bounded controls in Advances in Dynamic Games-Theory[M]", Switzerland: Birkhauser, Vol. 13, pp. 313-350, 2013.